ISSN 0030-400X, Optics and Spectroscopy, 2016, Vol. 121, No. 3, pp. 348–356. © Pleiades Publishing, Ltd., 2016.
Original Russian Text © G.V. Baryshnikov, V.A. Minaeva, B.F. Minaev, V.-H. Sun, M. Grigoras, 2016, published in Optika i Spektroskopiya, 2016, Vol. 121, No. 3, pp. 377–386.

CONDENSED-MATTER SPECTROSCOPY

Analysis of the Electronic, IR, and ^{1}H NMR Spectra of Conjugated Oligomers Based on 4,4'-Triphenylamine Vinylene

G. V. Baryshnikov[a], V. A. Minaeva[a], B. F. Minaev[a, b], V.-H. Sun[b], and M. Grigoras[c]

[a] *Bohdan Khmelnytsky National University of Cherkasy, 18031 Cherkasy, Ukraine*

[b] *Key Laboratory of Engineering Plastics and Beijing National Laboratory for Molecular Sciences, Institute of Chemistry, Chinese Academy of Sciences, Beijing, China*

[c] *P. Poni Institute of Macromolecular Chemistry, 700487 Iasi, Romania*

e-mail: glebchem@rambler.ru, bfmin@rambler.ru, minaeva@cdu.edu.ua

Received January 15, 2016

Abstract—Two types of conjugated oligomers based on 4,4'-triphenylamine vinylene have been synthesized and characterized by the methods of IR, UV–visible, and ^{1}H NMR spectroscopy. The corresponding spectra have also been simulated theoretically at the density functional theory level with application of the B3LYP and BMK hybrid exchange-correlation functionals. A comparative analysis of the experimental and theoretical spectra of polymers and oligomers has revealed regularities of the manifestation of spectral signals depending on the conjugation chain length and the presence of a substituent in the triphenylamine core. It has been established, in particular, that the absolute intensity of IR bands satisfies a linear dependence with increase in the degree of polymerization; however, no frequency shift is observed at the same time. The position of the main peak in electron absorption spectra demonstrates the bathochromic shift with an increase in the oligomeric chain length due to the narrowing of the energy gap between the boundary molecular orbitals. Based on the theoretical estimation of the hydrogen atoms chemical shifts, the signals of various protons types in the strongly broadened experimental ^{1}H NMR spectra of the bis-(4-iodine phenyl)-phenylamine and N,N-bis-(4-iodine phenyl)-4'-(phenylethynyl)-phenylamine polymerization products have also been identified.

DOI: 10.1134/S0030400X16090046

INTRODUCTION

Very rapid progress in the field of organic electronics has been observed in recent years, which is caused by the interest of humanity in the creation of alternative sources of electric energy and household lighting [1–4]. Conversion of solar electromagnetic radiation into electricity entails designing of photoelectric converters, the active media of which allow efficient electron transport during photoexcitation [4]. At the same time, the inverse phenomenon of electroluminescence has been successfully used for designing economical visible-light (including white light) sources [1–3, 5]. All these factors call for the creation of new organic materials allowing for photoelectro- and electrophotoconversion. These materials include π-conjugated oligomers and polymers based on 4,4'-triphenylamine vinylene [6]. They are characterized by high thermal stability, have large extinction coefficients at the absorption maxima (about 400 nm), and can fluoresce in various media. In addition, these polymers are favorable objects of "optical tuning" due to the possibility of functionalization of the initial monomers [6–8]. This allows one to vary the energy of the boundary molecular orbitals (MOs) and, accordingly, the absorption maximum in electron spectra of oligomers and polymers.

The introduction of highly polar substituents into the composition of polymers makes it possible, in particular, to observe solvatochromism in electron spectra when using solvents of different polarity [6]. Unfortunately, the theory of the electronic structure and spectra of oligomers based on 4,4'-triphenylamine vinylene has been poorly studied on the whole, although quantum-chemical calculations allow one to predict almost all physicochemical properties of molecules and even forecast the ways of forming materials with specified properties [9, 10]. In addition, spectroscopy of 4,4'-triphenylamine vinylene polymers is actually restricted to the analysis of IR absorption spectra, whereas electron absorption spectra and NMR spectra remain little-studied because of the difficulty in interpretation of spectral signals [6–8]. Therefore, quantum-chemical analysis of 4,4'-triphenylamine vinylene oligomer spectra is a convenient tool for interpreting observed polymer spectra.

In this study, we perform a comparative analysis of the experimental and theoretical IR, electron, and ^{1}H NMR spectra for two types of conjugated oligomers

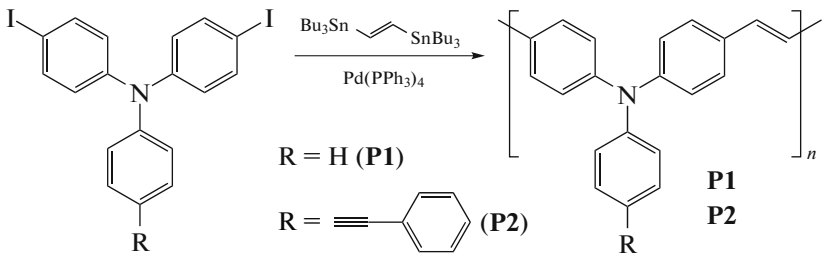

Fig. 1. Schematic diagram of the synthesis of polymers **P1** and **P2**.

based on 4,4'-triphenylamine vinylene in order to determine the dependence of the observed spectra on the presence of a substituent in the triphenylamine nucleus and the conjugation chain length. A solution of this problem provides possibilities for rational functionalization of oligomers and synthesis of new polymers for the field of organic electronics.

MATERIALS AND METHODS

Both types of 4,4'-triphenylamine vinylene polymers under consideration (referred to as **P1** and **P2** below) were obtained as a result of the Stille polycondensation reaction of iodine-derivative monomers bis-(4-iodine phenyl)-phenylamine and N,N-bis-(4-iodine phenyl)-4'-(phenylethynyl)-phenylamine (a general schematic diagram of the synthesis is shown in Fig. 1). The synthesis method and polymerization conditions were described in detail in [6–8]. The initial monomers for the synthesis of target polymers were prepared according to the technique described in [6] based on commercial reagents and catalysts produced by Aldrich and Fluka.

IR spectra of the synthesized polymers were measured in a potassium bromide matrix with a DIGI-LAB-FTS 2000 spectrometer in the frequency range of 4000–400 cm^{-1}. ^{1}H NMR spectra were measured using a Bruker Avance DRX-400 spectrometer with an operating frequency of 400 MHz in $CDCl_3$ solution. Chemical shifts were calculated with respect to the tetramethylsilane standard. Electron absorption spectra and fluorescence spectra of the solutions and solid films of polymers **P1** and **P2** were recorded by Specord 200 and Perkin Elmer LS 55 spectrometers, respectively. The solvent was chloroform, and quartz glass served as a substrate for thin polymer films.

CALCULATION METHOD

The procedure of optimizing the geometry of oligomers **P1** and **P2** (n = 1–5) was performed at the level of the density functional theory (DFT) using the hybrid exchange-correlation functional B3LYP [11, 12] in the basis 6-31G(d) [13]. A similar method was applied to calculate the IR absorption spectra of oligomers **P1** and **P2** (n = 1–5). To compare the calculated and experimental spectra, we used linear correction of the vibration frequencies in the form of a scaling factor equal to 0.969.

To analyze the electron absorption spectra of polymers **P1** and **P2**, we calculated 30 vertical singlet–singlet transitions for each oligomer (n = 1–5) within the method of time-dependent density functional theory (TD DFT) [14] using the Boese–Martin hybrid functional (BMK [15]), basis 6-31G(d), and the solvation polarizable continuum model (PCM) [16] (the solvent is chloroform).

The chemical shifts of hydrogen atoms were calculated within the gauge-invariant atomic orbital (GIAO) approximation by the DFT/B3LYP method using the extended thrice split valence basis 6-311++G(d,p) [17] with additional diffuse and polarization functions for hydrogen atoms (with respect to the TMS standard calculated by the same method).

A profile of the curves of the calculated electron and IR absorption spectra was constructed by the SWizard program [18] using the Gaussian distribution function for the electron spectra (the line half-width is 3500 cm^{-1}) and the Lorenz distribution function for the IR spectra (the line half-width is 10 cm^{-1}). The spectrum intensity was normalized to the common absorption maximum, which is assumed to be unity.

The band gap for polymers **P1** and **P2** was calculated by the B3LYP/6-31G(d) method with imposed periodic boundary conditions (PBCs) for the one-dimensional regular model of polymer.

All calculations by the DFT and TD DFT methods were performed within the GAUSSIAN 09 software package [19] on the PDC supercomputer at the KTH Royal Institute of Technology (Stockholm).

RESULTS AND DISCUSSION

*Electron Absorption Spectra of Oligomers **P1** and **P2***

Experimental spectra of the solutions of polymers **P1** and **P2** have similar form and contain two absorption bands: strong long-wavelength band in the visible range of 350–450 nm and weak band in the range of 275–350 nm [6]. The long-wavelength absorption band is due to the first and strongest $\pi\pi^*$-type electronic transition in the spectrum, which corresponds

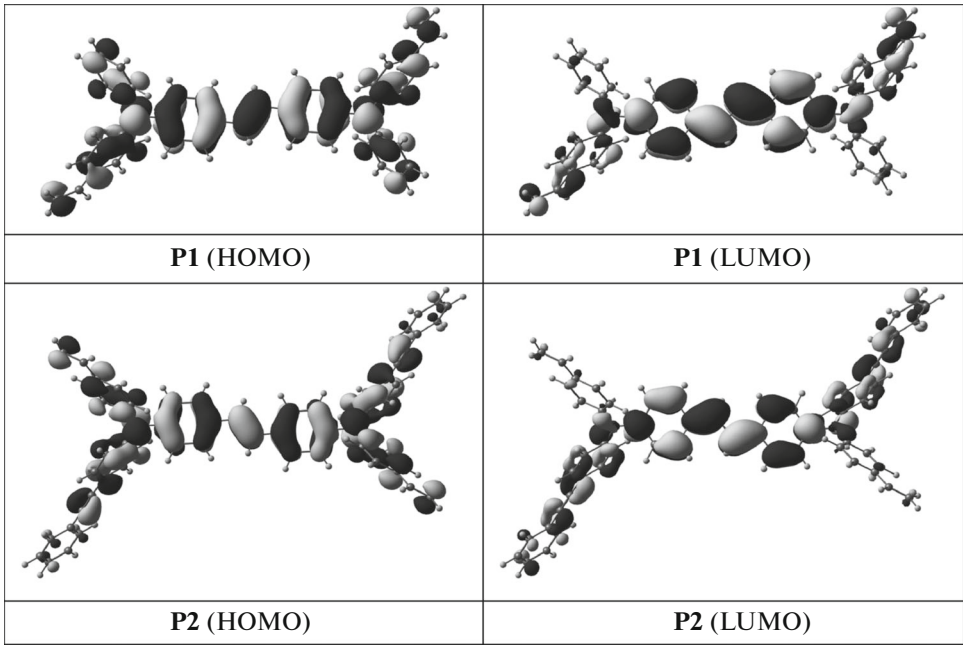

Fig. 2. Boundary MOs of oligomers **P1** and **P2** ($n = 2$).

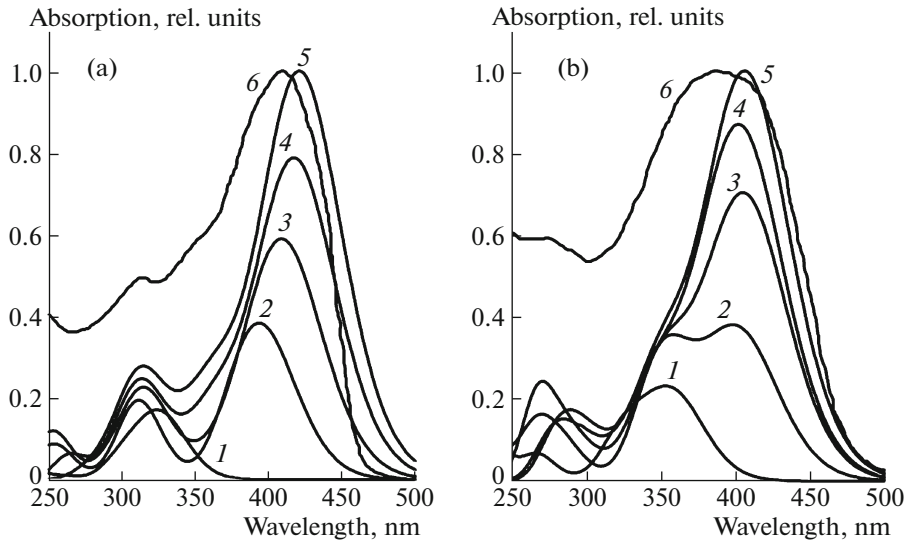

Fig. 3. Electron absorption spectra of oligomers (a) **P1** and (b) **P2**: (*1*–*5*) calculation by the TDDFT/B3LYP/6-31G(d) method taking into account the influence of the solvent for $n = 1$–5, respectively; (*6*) experimental spectrum of the polymer.

to single-electron excitation from the highest occupied molecular orbital (HOMO) to the lowest unoccupied molecular orbital (LUMO). For oligomers **P1**, this transition has a contribution of the electron-density transport from nitrogen atoms and phenyl fragments, which are not involved in conjugation between monomers, to the central conjugation chain (Fig. 2). In addition, the transition is accompanied by a radical change in the bonding–antibonding character with respect to double bonds (in both benzene rings and vinyl groups); i.e., the alternation of double and single bonds changes upon excitation into the first singlet in comparison with the ground state. All these factors cause an increase in the oscillator strength for the first electronic transition during the conjugation chain growth (Fig. 3, the table).

Similar conclusions are hold for oligomers **P2** as well: the first electronic transition has a contribution of the electron-density transport from terminal styrene fragments to the central conjugation chain, and

Energies of the boundary MOs of oligomers **P1** and **P2** in comparison with the energy and oscillator strength of the corresponding vertical $S_0 \rightarrow S_1$ transition

Oligomer	E(HOMO), eV	E(LUMO), eV	λ, nm	f	E(HOMO), eV	E(LUMO), eV	λ, nm	f
	P1				**P2**			
$n = 1$	−5.516	−0.276	328	0.98	−5.519	−0.772	360	1.35
$n = 2$	−5.312	−0.851	393	2.13	−5.360	−1.025	404	2.37
$n = 3$	−5.240	−0.956	411	3.13	−5.303	−1.072	413	3.09
$n = 4$	−5.209	−1.004	418	4.29	−5.273	−1.098	416	3.24
$n = 5$	−5.194	−1.028	422	5.38	−5.254	−1.105	418	3.43
$n = \infty$	−4.417	−1.564	–	–	−4.485	−1.633	–	–

the transition oscillator strength increases with an increase in n. Here, a bathochromic shift of the first absorption maximum due to the narrowing of the energy gap between the boundary orbitals is observed for both oligomer types, which can clearly be seen in Fig. 2 and the table. The shift value becomes less pronounced beginning with $n = 3$, and the calculated position of the absorption maximum is in good agreement with the experimental value (410 and 391 nm for **P1** and **P2**, respectively [6]). At the same time, the character of increase in the oscillator strength of the first electronic transition for oligomers **P1** and **P2** somewhat differs. In particular, the oscillator strength for oligomers **P1** increases linearly with an increase in n, which is described by the equation $f = 1.096n - 0.106$ with correlation coefficient $R^2 = 1$. For oligomers **P2**, the oscillator strength changes nonlinearly and can be represented in the best way as logarithmic dependence $f = 1.326(\ln n) + 1.426$ with confidence $R^2 = 0.98$.

Having calculated the energy of crystalline orbitals for the regular periodic structure of polymers **P1** and **P2**, we estimated the limiting values of the HOMO–LUMO energy gap (in fact, the band gap) to be 2.853 and 2.846 eV, respectively. These values of the band gap allow one to assign polymers **P1** and **P2** to wide-gap semiconductors. The dependences of the HOMO–LUMO gap width on the conjugation chain size are shown in Fig. 4.

Obviously, at small n values, the oligomers are typical insulators; however, the parameter of the HOMO–LUMO gap (HLG) tends to a limit in the region of semiconductor properties with an increase in n, which allows one to vary the polymer band gap depending on the degree of polymerization (the so-called "concept of HLG engineering"), i.e., to obtain materials with specified conductivity parameters. When passing from $n = 1$ to $n = \infty$, the parameters of the HLG value for compounds **P1** and **P2** are 2.39 and 2.60 eV, respectively, which are smaller than the initial HLG value at $n = 1$ by a factor of almost 2 (Fig. 4, table). This fact indicates about a significant change in the electronic structure of the molecules with an increase in n (specifically, growth of the conjugation chain and delocalization of the corresponding MOs). In this case, the ionization potentials decrease (growth of the HOMO energy) and the electron affinity increases (decrease in the LUMO energy), which is typical of polyenes and other conjugated π systems [20, 21].

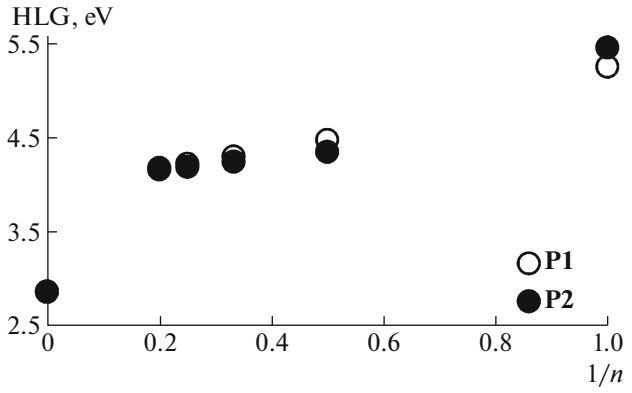

Fig. 4. Dependence of the energy gap between the boundary MOs on the degree of polymerization of compounds **P1** and **P2**.

*IR Spectra of Molecules **P1** and **P2***

The problem of calculating IR spectra of oligomers **P1** and **P2** is complicated to a great extent because by a significant increase in the number of atoms beginning with $n = 3$, which strongly increases the time of calculating second derivatives of the energy with respect to coordinates for the Hessian construction. At $n > 5$, the problem of calculating gradients, diagonalization, and further solution of the $(3N - 6)$-dimensional problem for harmonic oscillators (N is the number of atoms in the molecule; $N = 37$ and 49 for monomers **P1** and **P2**, respectively) within the B3LYP/6-31G(d) approximation becomes almost impossible for the available capability of the PDC supercomputer (Stockholm). However, an analysis of the spectra for $n = 2$–5 demonstrated a good reproducing of the

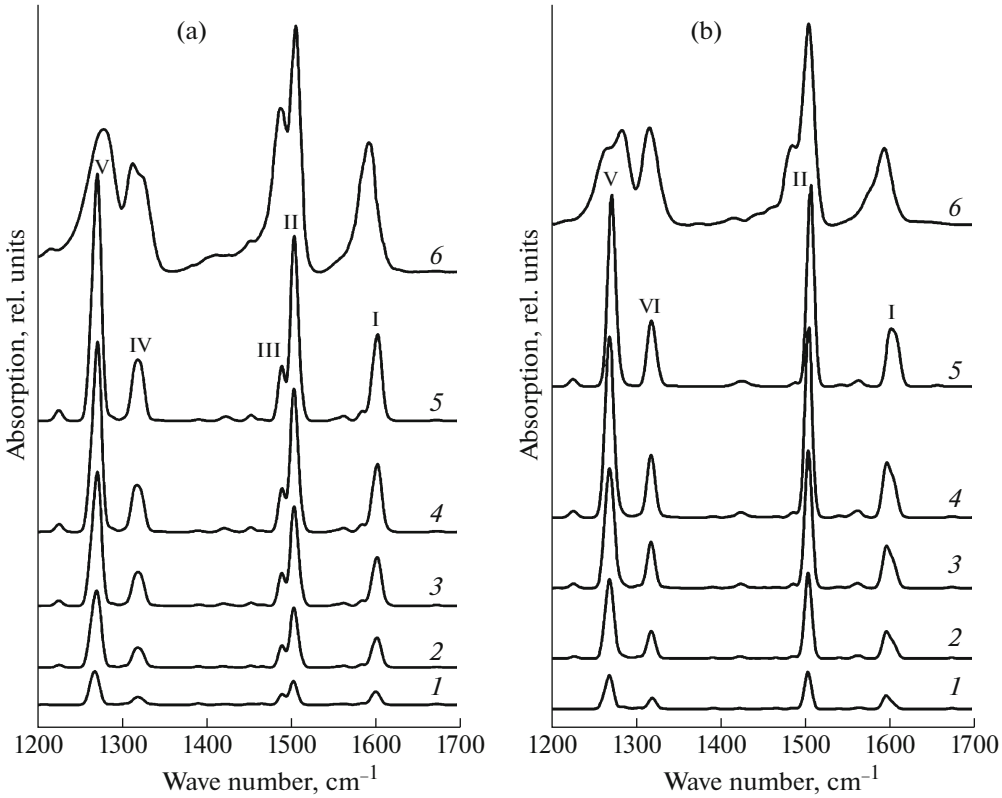

Fig. 5. Calculated IR spectra of oligomers (a) **P1** and (b) **P2** (curves *1–5*) in comparison with experimental curves *6*. The Roman numerals enumerate bands under consideration.

experimental curves and made it possible to determine the main tendencies in the IR spectra with an increase in n, which allows one to do without additional calculations of oligomers for $n > 5$ (especially taking into account a rather low experimental degree of polymerization of **P1** and **P2** ($n_{exp} = 13–15$) [6].

The calculated IR spectra of the compounds of monomers and oligomers **P1** and **P2** ($n = 2–5$) in the range of 1700–1200 cm^{-1} are presented in Fig. 5 and compared with the experimental IR spectra of the polymers. It can be seen that the calculated IR spectra are in good agreement with the experimental ones. All absorption bands are characterized by broadening and increase in the intensity with an increase in the number of the structural units (n). We found that the intensity of the absorption bands of oligomers **P1** and **P2** grows linearly with an increase in n (Fig. 6) due to the n-multiple degeneracy of the corresponding vibrational modes.

The intensity growth rate differs for the analyzed bands: bands II and V are amplified to a larger extent than the others because they initially have a high intensity (at $n = 1$), and the further n-multiple multiplication sharply increases the intensity. Similar conclusions are valid for bands I, III, and IV; however, the growth parameter of their intensity is smaller than that for bands II and V. Note that band III is present in the spectrum of oligomers **P2**; however, its intensity in the calculated spectra is very low, which does not make it possible to reliably analyze its intensity amplification parameters. It should also be noted that the occurrence of the phenylethynyl group in oligomers **P2** increases the absolute intensity of the bands having a contribution from the aromatic-ring vibrations. This fact can clearly be seen by the example of band I belonging to the stretching vibrations of C=C bonds of aromatic groups, the intensity of which in the spectra of oligomers **P2** increases more rapidly as compared with **P1**. The nature of bands I–V will be discussed in detail below (including an analysis of the other weaker bands).

Vibrations of the C_{benz}–N bonds of the triphenylamine fragment. We calculated vibrations of the C–N bond in the spectra of monomer **P1** and its oligomers in the ranges of 1615–1491, 1326–1321, and 1273–1265 cm^{-1}; they form the strongest bands in the IR spectrum. Strong absorption bands at 1504 cm^{-1} (band II with band III as a shoulder at 1491 cm^{-1}) and 1273 cm^{-1} (band V) is due to participation of the C–N bonds in asymmetric skeletal vibrations of the triphenylamine fragment. These peaks correspond to the bands at 1507 and 1280 cm^{-1} in the experimental spectrum of polymer **P1**. The absorption bands at 1604 cm^{-1} (band I) and 1316 cm^{-1} (band IV) (experi-

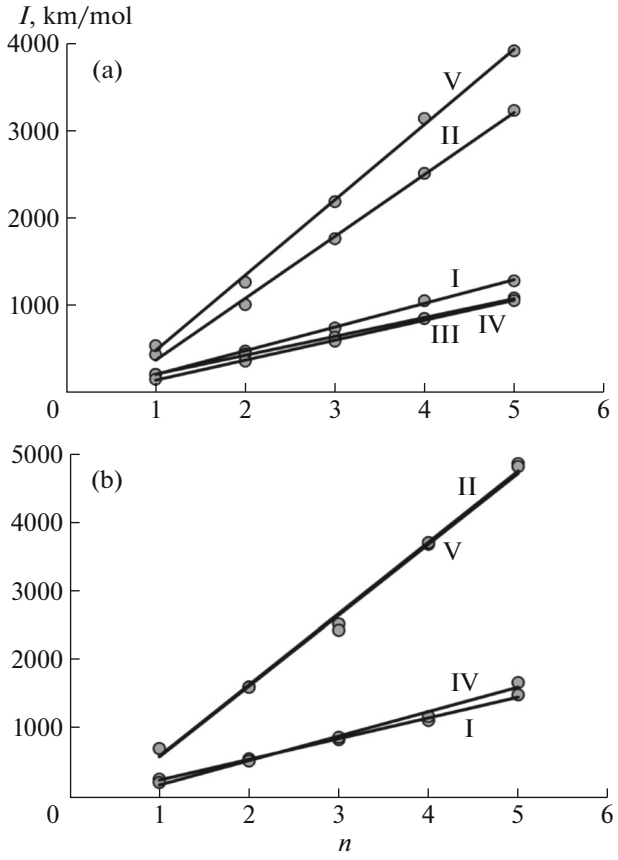

Fig. 6. Dependences of the IR band intensity on the size of oligomers (a) **P1** and (b) **P2**. The Roman numerals are denoted in Fig. 5.

mental bands at 1594 and 1314 cm^{-1}) have a contribution from the C–N bond absorption along with the absorption of the C=C bonds of aromatic rings. The νC–N bands in the IR spectrum of monomer and oligomers **P2** (Fig. 5b) are shifted by only 1–3 cm^{-1} in comparison with monomer and oligomers **P1**.

Vibrations of the CH aromatic cycles. Vibrations of the CH bonds in the IR spectra of aromatic compounds can be identified in the range of 3080–3010 cm^{-1} (νC–H), 1290–990 cm^{-1} (planar CH bending vibrations, δCH), and below 900 cm^{-1} (nonplanar CH bending vibrations, γCH) [22]. Stretching vibrations of the C–H bonds of benzene fragments have the highest frequency and form two weak bands at 3054 and 3022 cm^{-1} in the calculated IR spectrum of monomer **P1**; the corresponding bands in the experimental spectrum of the polymer are at 3058 and 3028 cm^{-1} (Fig. 1 in [6]). The νC–N bands in the IR spectrum of monomer and oligomers **P2** are shifted by only 1–3 cm^{-1} in comparison with monomer and oligomers **P1**.

Planar bending vibrations (δCH) are not mixed with vibrations of other types. They correspond to weak bands at 1178, 1106, 1073, and 1016 cm^{-1} in the experimental IR spectrum of polymer **P1** (Fig. 7a, curve *6*), which is in good agreement with the theoretical predictions for the monomer (1176, 1117, 1078, and 1023 cm^{-1}, Fig. 7a, curve *1*) and oligomers (Fig. 7a, curves *2–5*). The corresponding absorption bands in the experimental IR spectrum of polymer **P2** (Fig. 7b, curve *6*) are observed at the frequencies close to those for **P1**: 1178, 1103, 1071, and 1009 cm^{-1} (calculation for the monomer yields 1176, 1111, 1074, and 1021 cm^{-1}). Absorption at 1111 cm^{-1} in the calculated IR spectrum of monomer **P2** (Fig. 7b, curve *1*) makes a shoulder for the band at 1130 cm^{-1} belonging to the C_{benz}–C≡ bond vibration and also having a contribution from δCH vibrations. This band corresponds to the very weak band at 1140 cm^{-1} in the experimental spectrum of the polymer (Fig. 7b, curve *6*).

We calculated nonplanar CH bending vibrations of benzene fragments in monomers **P1** and **P2** in the range of 969–683 cm^{-1}. They correspond to the weak bands at 936, 839, 785, 748, 708, and 688 cm^{-1} in the IR spectrum of monomer **P1**. γCH bending vibrations calculated at 708 and 688 cm^{-1} are mixed with nonplanar bending vibrations of benzene rings. The corresponding absorption bands in polymer **P1** are observed experimentally at 959, 828, 802 (shoulder on the left), 755, 714, and 695 cm^{-1} (Fig. 7a, curve *6*). The corresponding γCH absorption bands in the IR spectrum of monomer **P2** are calculated at the frequencies close to those for **P1**: 936, 839 and 824 (doublet band), 785, 748, 715, and 683 cm^{-1}; in the experimental spectrum of polymer **P2**, these bands correspond to the absorption bands at 960, 826 (this asymmetric band can be considered as superposition of three calculated absorption bands at 839, 824, and 785 cm^{-1}), 754, 724, and 692 cm^{-1} (Fig. 7b, curve *6*).

Vibrations of the aromatic C=C bonds. Skeletal vibration bands of the aromatic C=C bonds in the IR spectra are generally observed in the range of 1650–1430 cm^{-1} [22, 23]. In the IR spectrum of monomer **P1** containing three benzene rings, symmetric νC=C vibrations form a mean-intensity band peaking at 1604 cm^{-1} (Fig. 5a, curve *1*, band I). This band corresponds to the absorption band at 1594 cm^{-1} in the experimental spectrum of polymer **P1** (Fig. 5a, curve *6*). Very weak absorption at 1421 cm^{-1} observed in the experimental spectrum of polymer **P1** (Fig. 5a, curve *6*) belongs to ν_{as}C=C vibrations (calculated value 1426 cm^{-1}). Asymmetric νC=C vibrations calculated for monomer **P1** at 1454 cm^{-1} do not form a significant absorption band in the IR spectra due to low intensity. The absorption band at 1316 cm^{-1} (band IV) in the IR spectra of monomer and oligomers **P1** (Fig. 5a, curves *1–5*) is formed by three normal vibrations with close calculated frequencies (1326, 1321, and 1316 cm^{-1}) and IR intensities of 70.1, 69.9, and 78.5 km/mol. Normal vibrations with the frequencies

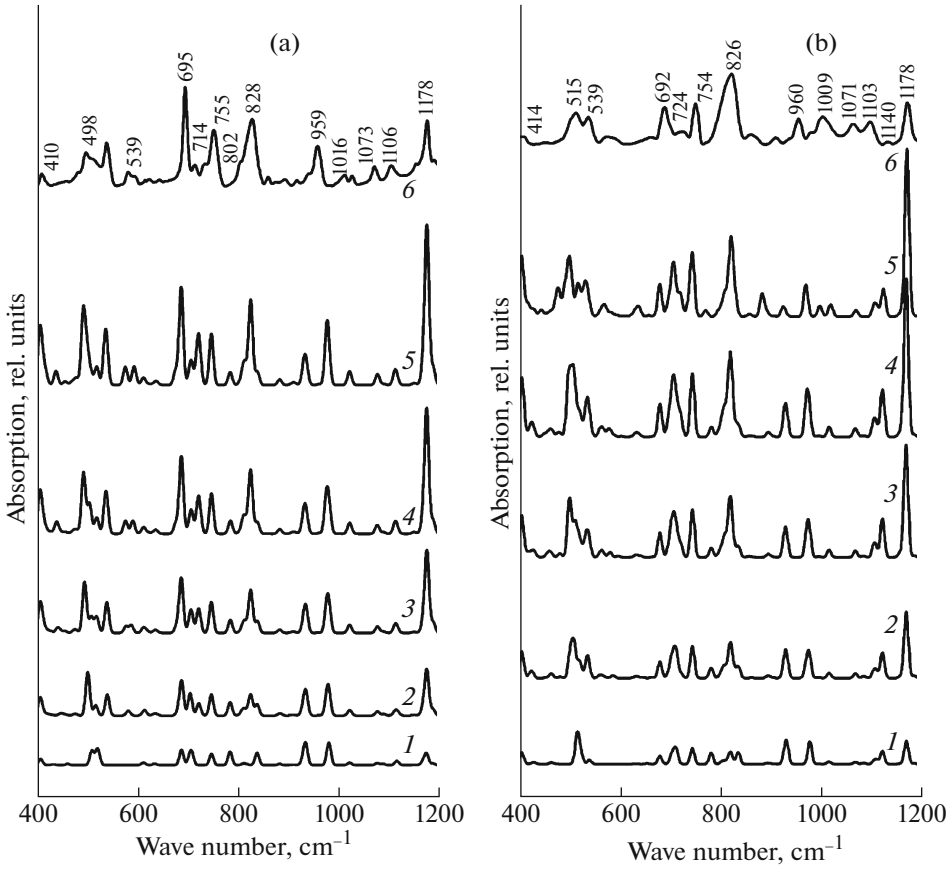

Fig. 7. Calculated IR spectra of oligomers (a) **P1** and (b) **P2** (curves *1*–*5*) in the frequency range of 400–1200 cm^{-1} in comparison with the experimental curves *6*. The intensities of the calculated spectra are given at a magnification of 5 times in comparison with Fig. 5.

of 1326 and 1321 cm^{-1} belong to C_{benz}–N bond vibrations of the triphenylamine fragment, which occur simultaneously with asymmetric vibrations of the aromatic νC=C bonds. Vibration with a frequency of 1316 cm^{-1} belongs to asymmetric C=C bond vibrations of benzene rings (Kekulé vibration). In the IR and Raman spectra of a free benzene molecule with symmetry D_{6h}, Kekulé vibrations (symmetry b_{2u}) are forbidden and not observed. In the experimental IR spectrum of polymer **P1**, a pronounced shoulder at 1328 cm^{-1} (Fig. 5a, curve *6*), corresponding to the theoretically calculated normal vibrations at 1326 and 1321 cm^{-1}, is observed near the band peaking at 1314 cm^{-1} (corresponding to the latter considered vibration) due to broadening of the absorption band.

The Kekulé vibration in the IR spectrum of monomer **P2**, containing four benzene rings, and its oligomers is observed at a lower frequency (1265 cm^{-1}) in comparison with **P1** (1316 cm^{-1}) and mixed with the C–N bond skeletal vibration, which changes the band shape: a shoulder at 1267 cm^{-1} arises on the left of the broadened band peaking at 1285 cm^{-1}.

Bending vibrations of aromatic rings. Bending vibrations of benzene rings in molecule **P1** calculated at 1292 and 1285 cm^{-1} are mixed with δCH vibrations of benzene fragments. They do not form separate bands in the calculated and experimental IR spectra because of low intensity (calculated *I* values are 4.6 and 6 km/mol, respectively). Planar bending vibrations of the rings at 1000 cm^{-1} in the range of 635–610 cm^{-1} (asymmetric bending vibrations) and at 914 and 909 cm^{-1} (symmetric bending vibrations) are characterized by even lower calculated absorption intensity. Nonplanar bending vibrations of benzene rings calculated in the ranges of 708–688 and 523–407 cm^{-1} have larger IR intensity and yield weak absorption bands at 695, 539, 498, and 410 cm^{-1} in the experimental spectrum of polymer **P1** (Fig. 7a, curve *6*). They also correspond to the weak bands at 692, 539, 515, and 414 cm^{-1} in polymer **P2** (Fig. 7b, curve *6*).

Vibrations of the C–H bonds of vinylene fragments. We calculated C–H bond vibrations of vinylene groups in monomers **P1** and **P2** and their oligomers in the range of 3000–2980 cm^{-1}. All C–H stretching

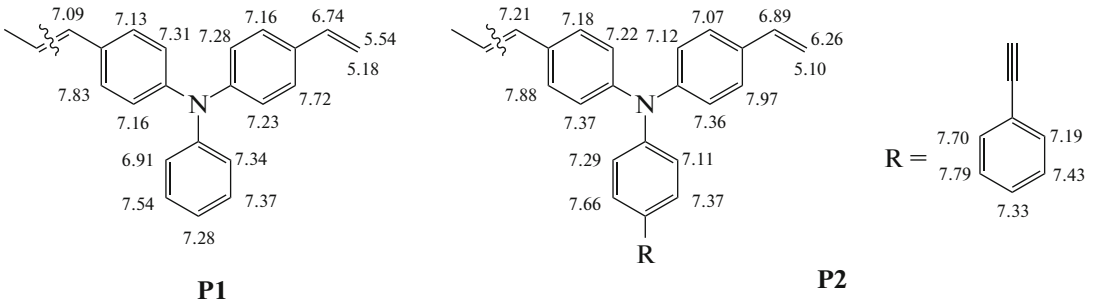

Fig. 8. Chemical shifts of hydrogen atoms calculated by the B3LYP/6-311++G(d,p) method for oligomers **P1** and **P2** ($n = 2$).

vibrations yield weak bands in the IR spectra of **P1** and **P2** [6].

We calculated planar bending vibrations of the CH bonds for a double bond in the range of 1337–1209 cm^{-1}. They are mixed with the δCH vibrations of benzene rings and do not form separate absorption bands. Absorption of the HC=CH nonplanar bending vibrations was calculated at 980 cm^{-1} (experimental values are 959 and 960 cm^{-1} for **P1** and **P2**, respectively) and is sufficiently strong to be observed in the IR spectrum (Fig. 7).

^{1}H NMR Spectra

One can select three main groups of hydrogen atoms in the structure of polymers **P1** and **P2** (Fig. 1), which belong to (i) CH bonds of aromatic cycles, (ii) CH bonds of *trans*-vinylene fragments, and (iii) CH bonds of CH_2 terminal groups. According to our calculation data (Fig. 8), hydrogen atoms of aromatic cycles yield characteristic signals in the range of 6.9–8.0 ppm, in complete agreement with the experimental data, which show the presence of a wide signal in the range of 6.5–8.0 ppm in the ^{1}H NMR spectra [6].

Signals of *trans*-vinylene protons were predicted by us to be in the same range (7.09 and 7.21 ppm for oligomers **P1** and **P2**, respectively; Fig. 8). The strong peak at 7.32 ppm in the experimental spectrum of polymer **P2** is most likely to belong to hydrogen atoms of *trans*-vinylene groups. At the same time, the signals of protons of CH_2 terminal groups are significantly shifted to the strong field and, according to the calculation data, occur in the range of 5.1–6.3 ppm. In the experimental spectrum of polymer **P2**, protons of this type correspond to the very weak signals at 5.15 and 5.67 ppm. Another weak signal at 6.6 ppm is likely to belong to the CH group bound with the CH_2 terminal group. In this case, the calculation predicts close to experimental values: 6.74 and 6.89 ppm for oligomers **P1** and **P2**, respectively (Fig. 8).

CONCLUSIONS

We analyzed the electronic, IR, and ^{1}H NMR spectra for two types of conjugated oligomers based on 4,4'-triphenylamine vinylene on the ground of experimental investigation results and quantum-chemical calculations. The oligomers under study were found to be characterized by size-dependent absorption in the visible spectral range due to narrowing of the energy gap between the boundary orbitals. Upon transfer to the periodic model of polymers, we observed even greater narrowing of the boundary orbitals, and the band gap decline down to about 2.85 eV, which corresponds to semiconductor properties of the polymers. Analysis of the IR spectra has shown that the absorption band intensity increases linearly with an increase in the degree of polymerization (n) due to n-multiple degeneracy of the corresponding vibrational modes without mixing with vibrations of other types. The strongest bands in the IR spectrum are determined by stretching vibrations of the C=C bonds of aromatic rings and the C–N bonds. Calculation of the chemical shifts of hydrogen atoms permits to find the assignments for the main signals in the experimental ^{1}H NMR spectra and, in particular, to identify weak signals of the terminal CH_2 groups, the concentration of which in the considered polymer samples is rather high, with account of the low degree of polymerization ($n_{exp} = 13–15$).

ACKNOWLEDGMENTS

One of the authors (M. Grigoras) thanks to the Romanian National Authority for Scientific Research (UEFISCDI) for financial support (Grant PN-II-ID-PCE-2011-3-0274, Contract 148/2011).

REFERENCES

1. S. Reineke, M. Thomschke, B. Lüssem, and K. Leo, Rev. Mod. Phys. **85**, 1245 (2013).
2. V. Cherpak, P. Stakhira, B. Minaev, G. Baryshnikov, E. Stromylo, I. Helzhynskyy, M. Chapran, D. Volyniuk, D. Tomkuté-Lukšiené, T. Malinauskas, V. Ge-

tautis, A. Tomkeviciene, J. Simokaitiene, and J. V. Grazulevicius, J. Phys. Chem. C **118**, 11271 (2014).

3. J.-H. Jou, R.-Z. Wu, H.-H. Yu, C.-J. Li, Y.-C. Jou, S.-H. Peng, Y.-L. Chen, C.-T. Chen, S.-M. Shen, P. Joers, and C.-Y. Hsieh, ACS Photon. **1**, 27 (2014).
4. A. Hagfeldt, G. Boschloo, L. Sun, L. Kloo, and H. Pettersson, Chem. Rev. **110**, 6595 (2010).
5. B. Minaev, G. Baryshnikov, and H. Agren, Phys. Chem. Chem. Phys. **16**, 1719 (2014).
6. M. Grigoras, A. M. Catargiu, T. Ivan, L. Vacareanu, B. Minaev, and E. Stromylo, Dyes Pigm. **113**, 227 (2015).
7. T. Ivan, L. Vacareanu, and M. Grigoras, Int. J. Polym. Mater. **62**, 270 (2013).
8. L. Vacareanu and M. Grigoras, High Perform. Polym. **23**, 112 (2011).
9. G. Baryshnikov, B. Minaev, N. Karaush, and V. Minaeva, RSC Adv. **4**, 25843 (2014).
10. G. Baryshnikov, B. Minaev, N. Karaush, and V. Minaeva, Phys. Chem. Chem. Phys. **16**, 6555 (2014).
11. A. D. Becke, Phys. Rev. A **38**, 3098 (1988).
12. C. Lee, W. Yang, and R. G. Parr, Phys. Rev. B **37**, 785 (1988).
13. M. M. Francl, W. J. Petro, W. J. Hehre, J. S. Binkley, M. S. Gordon, D. J. DeFrees, and J. A. Pople, J. Chem. Phys. **77**, 3654 (1982).
14. K. Burke, J. Werschnik, and E. K. U. Gross, J. Chem. Phys. **123**, 062206 (2005).
15. A. D. Boese and J. M. L. Martin, J. Chem. Phys. **121**, 3405 (2004).
16. S. Miertus, E. Scrocco, and J. Tomasi, Chem. Phys. **55**, 117 (1981).
17. K. Raghavachari, J. S. Binkley, R. Seeger, and J. A. Pople, J. Chem. Phys. **72**, 650 (1980).
18. S. I. Gorelsky, *SWizard Program* (Univ. Ottawa, Canada, 2010). http://www.sg_chem.net/.
19. M. J. Frisch, G. W. Trucks, H. B. Schlegel, G. E. Scuseria, M. A. Robb, J. R. Cheeseman, G. Scalmani, V. Barone, B. Mennucci, G. A. Petersson, et al., *Gaussian 09, Revision D.01* (Gaussian Inc., Wallingford CT, 2009).
20. B. S. Hudson, B. E. Kohler, and K. Schulten, Excited States **6**, 1 (1982).
21. K. N. Houk, P. S. Lee, and M. Nendel, Org. Chem. **66**, 5517 (2001).
22. G. Socrates, *Infrared and Raman Characteristic Group Frequencies—Tables and Charts,* 3rd ed. (Wiley, Chichester, 2001).
23. L. J. Bellamy, *The Infra-Red Spectra of Complexes Molecules* (Methuen, London, UK, 1954).